Received 1 March 2024; revised 28 March 2024; accepted 31 March 2024. Date of publication 4 April 2024; date of current version 27 May 2024.

Digital Object Identifier 10.1109/OJAP.2024.3385288

Integrated Solar Panel Slot Antennas Certified for CubeSat Missions

MAHMOUD N. MAHMOUD AND REYHAN BAKTUR (Senior Member, IEEE)

Department of Electrical and Computer Engineering, Utah State University, Logan, UT 84322, USA

CORRESPONDING AUTHOR: R. BAKTUR (e-mail: reyhan.baktur@usu.edu)

ABSTRACT This paper presents three prototypes of cavity-backed slot antennas integrated with solar panels. The antenna design is straightforward and requires minimal alteration on the solar panel's geometry. The antennas and solar cells are on the same surface and are effectively independent of each other. This eliminates the need for custom designed solar cells required in previous studies. The integrated solar panel antennas were demonstrated using all commercial-off-the-shelf space-qualified components and printed circuit board technology. The presented modular design method is valuable for CubeSats primarily built with standardized commercial components and where the surface area is limited to house solar panels and antennas separately. The integrated solar-antenna panels include a circularly polarized antenna, a linear two-slot antenna, and a dual band antenna. Measurements were performed to validate both antennas' and solar panels' functionality and the results are outstanding when compared to the antenna design data and solar cells' specifications.

INDEX TERMS Slot antenna, CubeSat, solar cell, integration.

I. INTRODUCTION

INTEGRATING antennas with solar cells have gained considerable interests in the last two decades. Co-sharing the surface area for solar cells and antennas is preferable for applications in wireless monitoring [1], remote self-powered sensors [2], aerospace vehicles [3], and small satellites [4]. Main interests in integrated solar cell antennas are the reduction of footprints and the feasibility of conformal mounting of the multifunctional solar-antenna panel on surfaces of spacecraft or monitors. Categorizing the reported literature as the location of the antenna with respect to solar cells, there have been studies where the antennas are integrated under [5], [6], [7], [8], [9], around [1], [2], and on top of the solar cells [10], [11].

Although there have been progress in designs and applications, including enhancing the antenna bandwidth and proposed use of the technology in the Internet of Things [12], [13], the reported designs often require custom-made solar cells or have complex integration geometry. This paper aims to present a simple and effective antenna design that can be integrated with commercial-off-the-shelf (COTS) solar cells and circuit boards.

Integrating antennas with solar cells without the need for custom designing the photovoltaic cells is highly appealing to CubeSat developers. A CubeSat is a miniaturized modular small satellite that conforms to specialized standards that specify its shape, size, and weight. The particular standards make it possible for companies to mass-produce components and offer COTS parts not only for CubeSats development but also for their transportation and launch [14], [15], [16]. Therefore, CubeSats have become low-cost space exploration and education platforms to teach, perform technology demonstrations, collect and analysis data such as space weather and Ionospheric scintillation. Figure 1 shows examples of recent CubeSats developed at Utah State University (USU).[1]

It is clear from Figure 1 that the majority surface, including the bottom side, of CubeSats are covered with solar cells. This is to ensure that the satellite has enough power, including when it is tumbling after being launched. It is therefore desirable not to remove any solar cell in order

[1]The size of a CubeSat is often characterized by the standard CubeSat "unit", U. A 1U CubeSat is a $10 \times 10 \times 10\,cm^3$ cube with a mass of approximately 1 to 1.33 kg. In the years since the CubeSat's inception, larger sizes have become popular, such as 2U, 3U, 6U, and 12U. There is also 0.5U CubeSat, which is half of a 1U, and accordingly there are 1.5U and 2.5U CubeSats too. A larger CubeSat has more science capability, but is more expensive. New configurations of CubeSats are always in development, depending on mission needs.

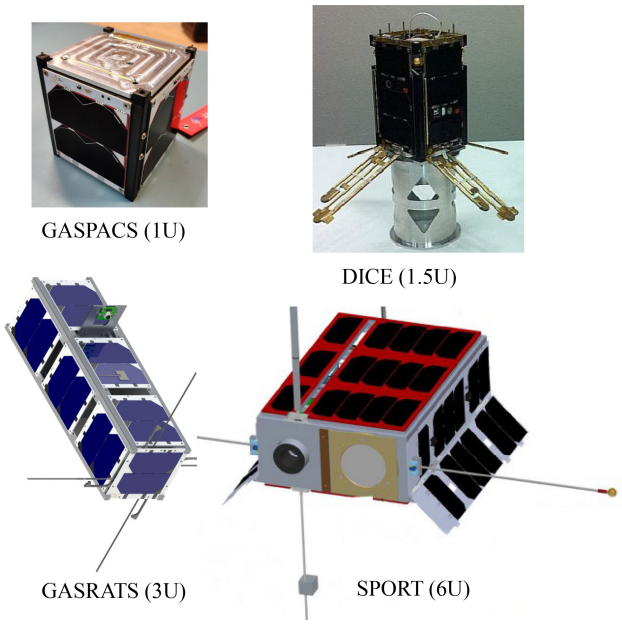

FIGURE 1. Recent CubeSat projects at USU.

to fit in a traditional antenna such as a patch. Deployable dipole antennas, although may not require considerable mounting areas as patches, have lower gain and therefore do not provide sufficient data rate needed for a fast downlink [17]. Accordingly, requirements for desirable antennas for CubeSats are summarized as follows.

1) The antennas should not compete for the surface real estate with solar cells.
2) The design method needs to be simple in order for in-house assembly with space-certified COTS solar cells and printed circuit board (PCB) technology.
3) The integrated solar cell antenna panel needs to be able to withhold thermal vacuum bake-out and vibration tests for a space deployment.

The objective of this paper is to present prototypes of integrated antennas that are ready for a 1.5U CubeSat mission, with all the space-mission requirements been verified.

II. METHODOLOGY

Based on the requirements listed in the introduction, a slot antenna geometry has been selected for the solar cell integration by considering the simplicity of the modular design, use of COTS parts, minimal alteration on the solar panel, and the least disturbance on the power generation. Other integration methods such as antennas placed under solar cells often requires custom-made solar cells [4] and an antenna placed on top of solar cells will impact the power generation even if the antenna is highly transparent unless the cover glass where the antenna is printed on is extremely transparent [18], which is limited by the material development and a suitableness for space deployment. Slot

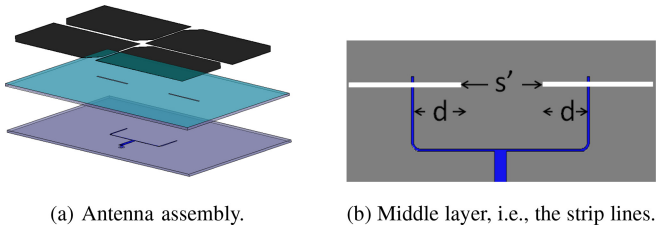

(a) Antenna assembly. (b) Middle layer, i.e., the strip lines.

FIGURE 2. Geometry of two cavity-backed slot antennas.

antennas, on the other hand, have low profile and can be inserted between solar cells or around them.

A slot created on a ground plane can be a complementary dipole antenna [19]. When not backed by a cavity, it radiates to both sides of the ground plane. In applications such as solar panel integration, it is important to limit the radiation to only the front side of the slot by utilizing a cavity backing [20], [21], [22]. The cavity can be loaded with dielectrics to modify the antenna, such as enhancing the impedance bandwidth or reducing its size.

Practical aspects of the dielectric loading of the cavity include the structural steadiness and the convenience to use a PCB to function as the cavity for the slot antenna. It is noted that most CubeSats use PCB to house solar cells. Accordingly, the proposed antennas utilize two pieces of PCB to create the radiating slot and the feed line.

A. ANTENNA GEOMETRY

The configuration of the cavity-backed slot antenna is shown in Figure 2. The antenna and the feed lines are composed of two circuit board substrates (Figure 2(a)). Two radiating slots are etched on the top layer, which is a conductor (copper in this case) layer, of the first substrate. The feed lines are printed on the top layer of the second substrate (Figure 2(b)). The bottom layer of the second substrate is the ground plane. The two substrates are then assembled together with antennas on the topmost layer and the feed lines sandwiched between the two substrates. The antenna elements are designed and assembled to be orthogonal to the feed lines (Figure 2(b)). It should be noted that one does not have to choose the same substrates to etch antennas and to print feed lines. Also, depending on applications and practical demands, the excitation method can be a simple probe feed [23], coplanar waveguide (CPW) feed [24], or microstrip line feed [19], [25], [26]. This paper demonstrates the strip line feed due to its simplicity and the ease in matching the lines to the slot antenna by adjusting the position and length of the feed lines. It should be noted that since the feed line is sandwiched between two substrates backed by ground planes, the line needs to be modeled as strip lines. After assembling the two substrates, the four sidewalls of the substrates and the top plane (i.e., slot antenna and the metal plane) are shorted to the ground plane with either conductive paste or plating.

In order to secure the shorting of side walls, vias may be utilized, as long as they do not interfere with the radiating

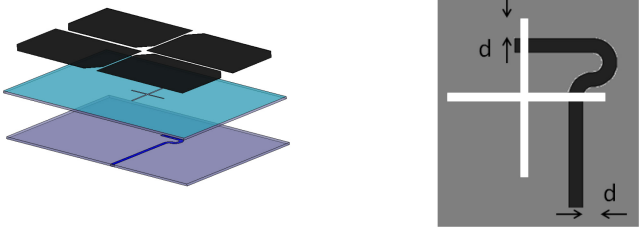

(a) Antenna assembly. (b) Feed design.

FIGURE 3. Layout of the circularly polarized cavity-backed slot antenna.

slots nor short the feed-lines to the ground. The width of the strip lines are calculated to provide needful impedance (e.g., in Figure 2(b), a 50 Ω line for the connector branches into two 100 Ω lines to feed the slots). The length of the slot is half wavelength (denoted as λ) in the effective dielectric that is a weighed average of the PCB substrate and air [27], and the width is narrow and determined by considering the available space and fabrication tolerance. Although wider slots have shown to improve impedance bandwidth [26], the geometry is not practical considering the limited space between solar cells. The impedance of a slot antenna is the highest at the center and lowest at the end-points of the slot. Accordingly the impedance matching for the slot is achieved by adjusting the offset (d in Figure 2(b)) of the feed line.

B. CIRCULAR POLARIZATION AND DUAL BAND DESIGN

Circular polarization (CP) is favored in satellite communication as it helps to simplify the ground station design, or in another language, reduces polarization loss [17]. There are many well established methods to achieve CP. This project chose a simple scheme by exciting two orthogonal identical slot with a 90° phase off-set (Figure 3). The layer information, slot dimension, impedance matching, and the PCB assembly are the same as in Section II-A. The required phased off-set for CP is achieved by adjusting the bent portion in the feed line design (Figure 3(b)).

It has been demonstrated that when the spacing between the two linear slots (S' in Figure 2(a)) is closer than 0.2λ, one could achieve an effective dual band antenna by adjusting the spacing and impedance matching [28]. A dual band antenna array design is demonstrated as shown in Figure 4 with the same PCB assembly as discussed in previous two sections. The feed design is to have an 50 Ω SMA connector at the center of the panel and use a half wavelength taped line to transform the impedance to 25 Ω. The 25 Ω line is then split to two 50 Ω lines and the rest is the same as in Section II-A.

III. PROTOTYPES

Because the antennas and solar panels are intended for a near-future space application, the criteria for the PCB material selection includes excellent tensile strength, thermal

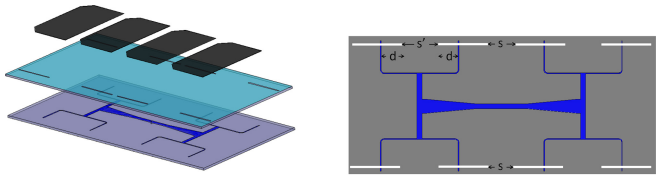

(a) Antenna assembly. (b) Feed design.

FIGURE 4. Layout of the dual band linear slot antenna.

TABLE 1. Design parameters.

Parameters	Linear Slots (Figure 2)	CP Slots (Figure 3)	Dual Band Slots (Figure 4)
Panel Size (mm^2)	155 × 96	155 × 96	190 × 96
CubeSat Fit (U)	1.5	1.5	2
Slot length (mm)	33.4	28	35
Slot width (mm)	1	1	1
d (mm)	2.25	2	5.75
s' (mm)	40	-	42
s (mm)	-	-	2

stability, resistance to outer space particles, very low extension coefficient in extreme temperature, and low outgassing.[2] Based on these requirements and an easy production at a PCB board house, a filled Polyimide was chosen as the substrate for the slot antenna. The Polyimide has a high relative permittivity of 5 and loss tangent of 0.03∼ 0.04. This results in a lower antenna efficiency (40% ∼ 60%) at S band. But the material still stood out as a top choice when considering application environment and cost.

Three antennas with geometry as shown in Figures 2-4 were designed using Ansys' HFSS, and the design parameters are summarized in Table 1.

A. FABRICATION

The antennas were fabricated with the standard masking and etching PCB manufacturing method according to the parameters in Table 1. A three-layer PCB board with layer geometry as shown in Figure 5 was produced. In the picture, the black part is metal (i.e., copper) and the white part is the result of etching. As seen, the top layer has the slot antennas as well as the traces for solar cells etched on. The middle layer is the metallic feed lines, and the bottom layer houses etched traces for surface-mount connectors for the antenna and solar panel. All three antennas were produced on one PCB board, and then the board was cut to yield three panels. As explained in Section II-A, the walls of the antenna-solar panel needs to be shorted. This was done by plating metallic coating on the walls at the PCB production facility. To ensure

[2]CubeSats are often launched by sharing the rocket with other expensive space cargo. It is important that they do not let out any substance that may contaminate other instruments. Outgassing refers to the sublimation or evaporation of materials as those materials are taken to a high-vacuum environment like space. Material used for space mission is required to have low outgassing level and be baked in a thermal vacuum chamber to ensure that any matter that would have been released during launch is safely released in the bake-out [29].

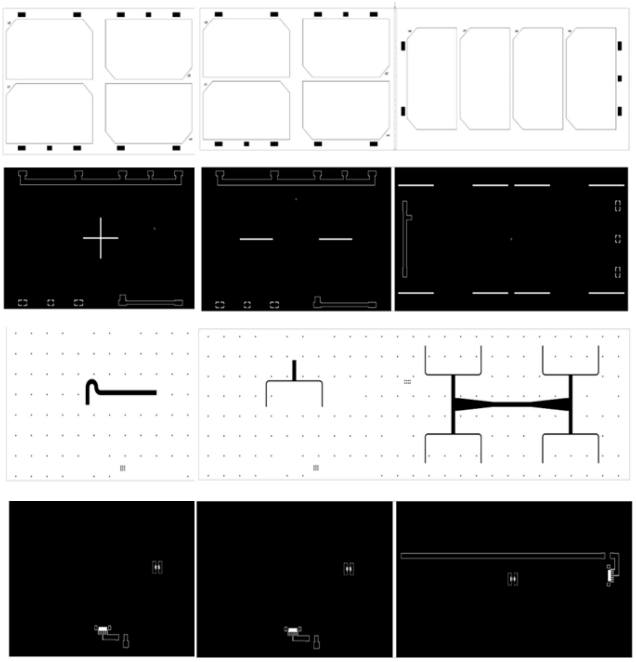

FIGURE 5. PCB layers of the slot antennas.

the grounding of the top and bottom layers, vias (Figure 5, little dots in the middle layers) were created to connect the two layers. In this prototype, vias were uniformly placed with a $\lambda/4$ separation. It should be noted that vias are optional, and a wider separation or placing them only next to the walls is acceptable.

B. INTEGRATION WITH SOLAR CELLS

After the antenna production, triple junction GaAs solar cells with 30% efficiency from AZUR SPACE [30] were integrated on the top layer of the PCB panels using space-grade adhesive. Each solar cell has a dimension of 39.7×69.13 mm^2 and outputs an average open circuit voltage and short circuit current of 2.69 V and 456.5 mA. The solar cells were connected in series to output a minimum 10 V open circuit voltage. The attachment process was enhanced in a vacuum chamber to ensure effective connections. Figures 6-8 are the fabricated solar panel antenna prototypes. Due to the cost of space solar cells, the linear slot antenna panel did not receive an integration. Performance of this antenna in the presence of the solar cells can be deduced and correlated from the measurements of the other two panels.

IV. MEASUREMENTS AND DISCUSSIONS

The integrated solar panel slot antennas were validated for return loss, radiation patterns, gain, and efficiency before and after the integration with solar cells, except for the linear slot antenna that was measured without solar cells. The results are summarized in Figures 9-16. The simulation results were performed for PCB assembly without solar cells because in this type of integration, the antenna is considered to be independent from the solar cell geometry, unlike the other

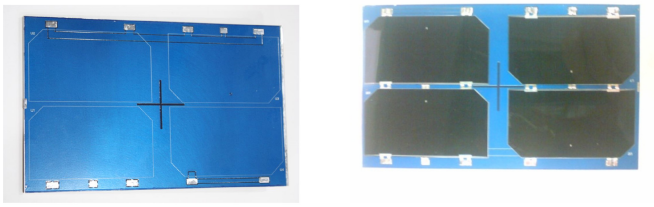

(a) CP slot prototype. (b) Integration with solar cells.

FIGURE 6. CP slot antenna integrated with solar cells.

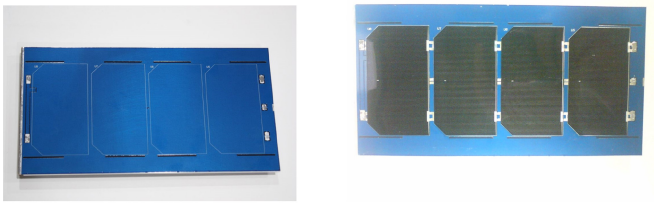

(a) Antenna prototype. (b) Integration with solar cells.

FIGURE 7. Dual band slot antenna integrated with solar cells.

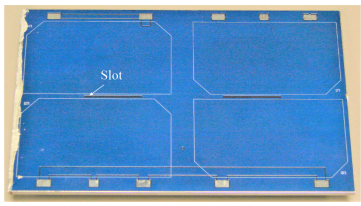

FIGURE 8. Linear slot antenna prototype.

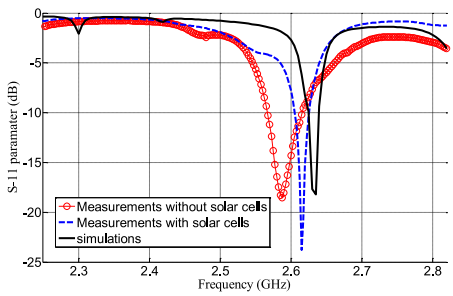

FIGURE 9. Reflection coefficient of the CP slot antenna.

types of integration where solar cell can be part of the ground plane [18].

Because the CP (Figure 6) and linear slots (Figure 8) resides at the center of the solar panel, it can be expected the antennas have low back lobe level. Therefore the pattern measurements for these two panels were performed only for the front hemisphere. Comparing the full pattern measurement (Figure 14) for the dual band slot antenna with the front-hemisphere pattern (Figure 13), it is clear that scanning the half hemisphere is sufficient to validate antennas' effectiveness and the effect of integration. It is seen that moving the slot from the center of the panel (e.g., linear and CP slots) to the edge (e.g., dual band slots) shifts the null of the E plane pattern, which is

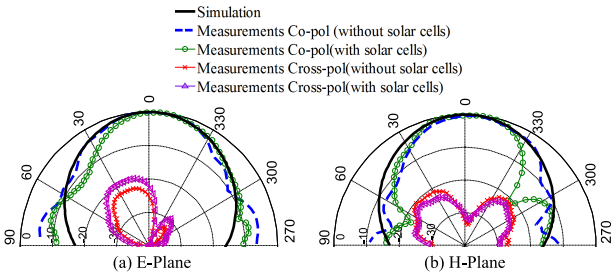

FIGURE 10. Radiation pattern of the CP slot antenna.

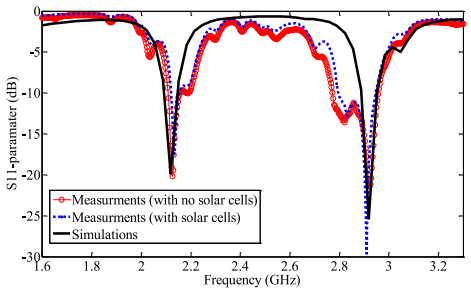

FIGURE 11. Reflection coefficient of the dual band antenna.

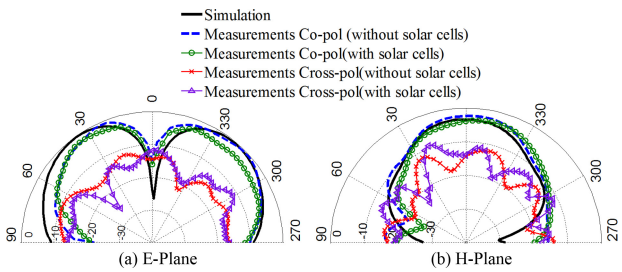

FIGURE 12. Radiation pattern of the dual band antenna at the lower band.

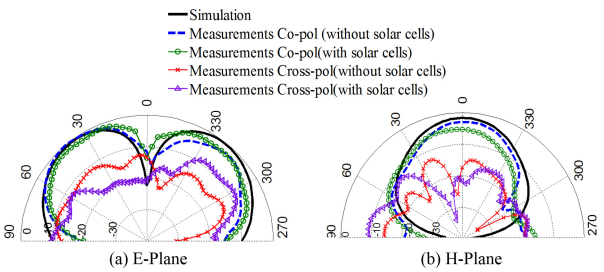

FIGURE 13. Radiation pattern of the dual band antenna at the upper band.

understandable from the antenna geometry. This information is useful in deploying these integrated antennas with small satellites when calculating pointing loss in the link budget [17].

For the antenna in Figure 6, the axis ratio (AR) was measured to ensure the effectiveness of the CP. The minimum AR of 0.6 dB was achieved at the main bream, and the AR remained less than 3 dB for within ±15° from the main beam. These results are comparable with typical microstrip patch antenna, and the antenna is deemed as providing a sufficient CP.

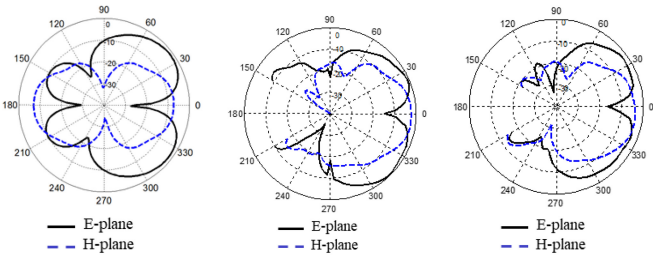

FIGURE 14. Full elevation plane radiation patterns of the dual band antenna at 2.9 GHz (upper band).

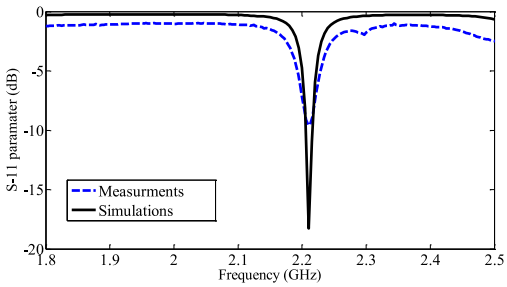

FIGURE 15. Reflection coefficient of the linear slot antenna.

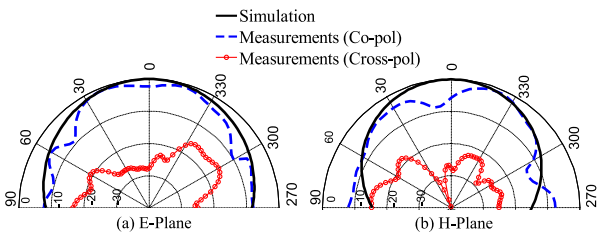

FIGURE 16. Radiation pattern of the linear slot antenna.

A. ANTENNA PERFORMANCE

From the measured results, it is seen that the performance of the antennas matched notably well with the simulated results. There is no discernible effect in the antennas' behavior after the integration of solar cells. It is seen from Figures 9, 11, and 15 that the impedance matching of the antenna remained sufficient after the PCB production process, and is somewhat enhanced by the solar cells. This is likely due to the metallic bottom layer of the solar cells, that effectively enhanced the ground plane for the slot antenna. It is also seen that the solar cell's metallic layer sharpened the E-plane radiation patterns of the antenna slightly, which is understandable considering the boundary condition for electric field at the near-by electric conductors. But that effect is small and is negligible to the antenna's gain and efficiency. The shift in the frequency between simulation, prototype, and integration of solar cells is more visible in Figure 9 than other panels. The shift between the simulation and prototype without solar cell is largely due to the fabrication tolerance, adhesive layer to bond the PCB, and the soldering of the connector through vias. This shift has been observed in Figure 11 and

TABLE 2. Realized efficiency and gain.

Antenna	Efficiency	Gain
Linear (Figure 2)	60%	3.9 dBi
CP (Figure 2)	54%	2.8 dBic
Dual Band (low) (Figure 4)	60%	2.2 dBi
Dual Band (high)	52%	3.4 dBic

[h]

in similar antenna designs [28]. The more visible shift after the integration of solar in Figure 9 is because in the CP antenna assembly (Figure 6), the tips of one of the slots are at the near vicinity of the metallic connectors of solar cells, which could have made the slot appear to be "shorter" and accordingly operate at a slightly higher frequency. Such an effect is not observed in assembly such as Figure 7 where the slot is placed slightly away from the solar cell. Above all, it should be noted that the shift is less than 2% from the design frequency, and the antenna design can be deemed independent from the solar cells as long as the solar cell and its connection do not touch or overlap the slot antenna.

Although solar cells have been shown to be a lossy material [18], the coupling with the solar cells has been observed marginal for the slot antenna integration as long as the antenna is not at the immediate vicinity of the cells. The realized gain and efficiency were measured and summarized in Table 2. It is seen that the efficiency is consistent with the ones computed from the loss tangent of the PCB substrate and is not affected by the solar cells. The measured gains were consistent with the geometry of the antennas. The CP and linear slots are at the center of the panel and have a larger ground plane and therefore the directivity of the two are close to 5 and 7 $\sim$ 8 dB respectively. The dual band slots are close to the edge of the panel and therefore has lower directivity, with upper band having slightly higher value because of the number of radiating elements.

B. SOLAR CELL PERFORMANCE

It is expected that the antennas would not affect the behavior of solar cells since the antennas are effectively independent of the solar cells assembly and connection. To verify the prediction and to document the solar panel's functionality, the panels were measured both in a controlled photovoltaic test bench and outside on a clear and sunny noon. The results were consistent. Before a test, the solar cells were cleaned with alcohol and an ionizer was turned on near the test bench for air purifying. The measurement setup on the test bench consists of artificial light, pyrometer, computer-controlled variable resistor, and multimeter. The measured power and current with respect to the output voltage are plotted in Figure 17. It is clear that maximum open circuit voltage is a bit over 10 V as expected. The maximum power output by the solar panel was measured to be 3.6 W, and can be verified by multiplying the current and voltage readings in Figure 17. The illuminated power from the artificial light was measured with the pyrometer to be 12.15 W. Therefore

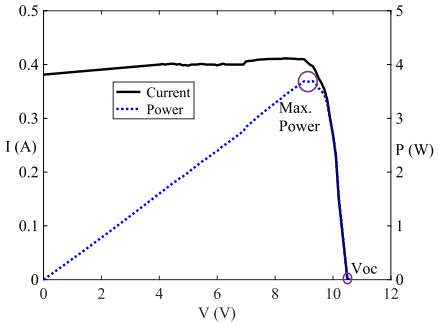

FIGURE 17. Measured I-V curve of the solar panel.

the efficiency of the solar cell is calculated to be $3.6/12.15 = 29.6\%$, which is an outstanding match with the factory data.

C. EFFECT OF VIAS

As presented in the fabrication section, vias were created to ground the top and bottom layer in addition to shorting the walls for slot antennas to function as designed. It was observed that as long as the vias were spaced for no less than $\lambda/5$ at the lowest operational frequency, there is not any visible effect on the antennas. This is because these antennas operate at S band and the size of vias is much smaller, and the spacing is not enough to create a cavity (like a Faraday cage) around the slots. Vias could affect the antennas for frequencies higher than X band and one should avoid putting them near the slots. Vias are not necessary, but since producing them is easy with PCB methods, they can be effective tools to create the ground for the slot antenna. At higher frequencies, instead of distributing vias evenly as in this project, they can be placed near the walls in order not to affect the antenna.

V. CONCLUSION

A straightforward and effective method for integrating conformal antennas with solar cells is presented. The antenna design is based on cavity-backed slots and can be placed around solar cells without interacting with them. The modular fashion of the antenna design facilitates the feasibility of using COTS solar cells and PCB technology, therefore reducing production complexity and cost. Three designs were demonstrated and validated for both antennas' and solar cells' functionality. The measured results matched design data very well and it has been observed that the interaction between the antennas and solar cells is minimal.

The proposed design and integration method is adaptable for many applications where surface area is limited, and is particularly beneficial for CubeSat missions. All material used for the integrated solar cell antenna panel is space-qualified and the design is ready to replace the S band patch down-link antennas, which uses at least the area of two solar cells on CubeSats. It should be noted that most educational CubeSats are small and often 1U. In order to have sufficient power, the developers are forced to sacrifice the down-link data rate by using the deployable UHF antennas. The

presented designs can be an immediate solution for those small spacecraft, and can be used in array configurations for higher gain on larger satellites. The panels fabricated were for 1.5 U and 2U CubeSats and can be used in larger CubeSats without any alteration. For a 1U CubeSat use, four smaller solar cells (e.g., 40×40 mm^2 cells [30]) could be used to house the cross slot at the center. The slot antenna geometry can also be scaled for higher frequencies and modified into designs such as meander line or square loop to reduce the size or produce CP.

REFERENCES

[1] O. O'Conchubhair, P. McEvoy, and M. J. Ammann, "Integration of antenna array with multicrystalline silicon solar cell," *IEEE Antennas Wireless Propag. Lett.*, vol. 14, pp. 1231–1234, 2015.

[2] T. Wu, R. Li, and M. M. Tentzeris, "A scalable solar antenna for autonomous integrated wireless sensor nodes," *IEEE Antennas Wireless Propag. Lett.*, vol. 10, pp. 510–513, 2011.

[3] J. Oh, K. Lee, T. Hughes, S. Forrest, and K. Sarabandi, "Flexible antenna integrated with an epitaxial lift-off solar cell array for flapping-wing robots," *IEEE Trans. Antennas Propag.*, vol. 62, no. 8, pp. 4356–4361, Aug. 2014.

[4] S. Vaccaro et al., "In-flight experiment for combined planar antennas and solar cells (SOLANT)," *IET Microw., Antennas Propag.*, vol. 3, no. 8, p. 1279–1287, 2009.

[5] S. Vaccaro et al., "Integrated solar panel antennas," *Electron. Lett.*, vol. 36, no. 5, p. 390, 2000. [Online]. Available: https://doi.org/10.1049/el:20000350

[6] S. Vaccaro et al., "Stainless steel slot antenna with integrated solar cells," *Electron. Lett.*, vol. 36, no. 25, p. 2059, 2000. [Online]. Available: https://doi.org/10.1049/el:20001467

[7] S. Vaccaro et al., "Combination of antennas and solar cells for satellite communications," *Microw. Opt. Technol. Lett.*, vol. 29, no. 1, pp. 11–16, Feb. 2001. [Online]. Available: https://doi.org/10.1002/mop.1068

[8] S. Vaccaro, J. Mosig, and P. De Maagt, "Two advanced solar antenna "SOLANT" designs for satellite and terrestrial communications," *IEEE Trans. Antennas Propag.*, vol. 51, no. 8, pp. 2028–2034, Aug. 2003.

[9] S. X. Ta, J. J. Lee, and I. Park, "Solar-cell metasurface-integrated circularly polarized antenna with 100% insolation," *IEEE Antennas Wireless Propag. Lett.*, vol. 16, pp. 2675–2678, 2017.

[10] S. V. Shynu, M. J. Roo Ons, P. McEvoy, M. J. Ammann, S. J. McCormack, and B. Norton, "Integration of microstrip patch antenna with polycrystalline silicon solar cell," *IEEE Trans. Antennas Propag.*, vol. 57, no. 12, pp. 3969–3972, Dec. 2009.

[11] T. W. Turpin and R. Baktur, "Meshed patch antennas integrated on solar cells," *IEEE Antennas Wireless Propag. Lett.*, vol. 8, pp. 693–696, 2009.

[12] W. An, H. Wang, J. Wang, Y. Luo, K. Ma, and J. Ma, "Low-profile wideband microstrip antenna integrated with solar cells," *IEEE Trans. Antennas Propag.*, vol. 70, no. 9, pp. 8530–8535, Sep. 2022.

[13] H. Wang, Y. B. Park, and I. Park, "Low-profile wideband solar-cell-integrated circularly polarized cubesat antenna for the Internet of Space Things," *IEEE Access*, vol. 10, pp. 61451–61462, 2022.

[14] "Cubesat design specification rev. 13." cubeSat. [Online]. Available: https://www.cubesat.org/resources

[15] S. Gao, M. Sweeting, S. Nakasuka, and S. Worden, "Special issue: Small satellites," *Proc. IEEE*, vol. 106, no. 3, 2018, pp. 339–342.

[16] Y. Rahmat-Samii, "Special issue on antenna innovations for cubeSats and smallSats," *IEEE Antennas Propag. Mag.*, vol. 58, no. 2, pp. 123–123, Apr. 2016.

[17] R. Baktur, "CubeSat link budget: Elements, calculations, and examples," *IEEE Antennas Propag. Mag.*, vol. 64, no. 6, pp. 16–28, Dec. 2022.

[18] T. Yekan and R. Baktur, "Study of the impact between a triple junction space solar cell and the antenna integrated on top of it," *IEEE Trans. Antennas Propag.*, vol. 69, no. 3, pp. 1734–1739, Mar. 2021.

[19] Y. Yoshimura, "A microstripline slot antenna (short papers)," *IEEE Trans. Microw. Theory Techn.*, vol. 20, no. 11, pp. 760–762, Nov. 1972.

[20] A. Adams, "Flush mounted rectangular cavity slot antennas–theory and design," *IEEE Trans. Antennas Propag.*, vol. 15, no. 3, pp. 342–351, May 1967.

[21] C. Cockrell, "The input admittance of the rectangular cavity-backed slot antenna," *IEEE Trans. Antennas Propag.*, vol. 24, no. 3, pp. 288–294, May 1976.

[22] S. Long, "Experimental study of the impedance of cavity-backed slot antennas," *IEEE Trans. Antennas Propag.*, vol. 23, no. 1, pp. 1–7, Jan. 1975.

[23] D. Sievenpiper, H.-P. Hsu, and R. Riley, "Low-profile cavity-backed crossed-slot antenna with a single-probe feed designed for 2.34-Ghz satellite radio applications," *IEEE Trans. Antennas Propag.*, vol. 52, no. 3, pp. 873–879, Mar. 2004.

[24] S. Sierra-Garcia and J.-J. Laurin, "Study of a CPW inductively coupled slot antenna," *IEEE Trans. Antennas Propag.*, vol. 47, no. 1, pp. 58–64, Jan. 1999.

[25] B. Zheng and Z. Shen, "Effect of a finite ground plane on microstrip-fed cavity-backed slot antennas," *IEEE Trans. Antennas Propag.*, vol. 53, no. 2, pp. 862–865, Feb. 2005.

[26] L. Zhu and K. Wu, "Complete circuit model of microstrip-fed slot radiator: Theory and experiments," *IEEE Microw. Guid. Wave Lett.*, vol. 9, no. 8, pp. 305–307, Aug. 1999.

[27] C. A. Balanis, *Antenna Theory: Analysis and Design*. New York, NY, USA: Wiley, 2016.

[28] M. N. Mahmoud and R. Baktur, "A dual band microstrip-fed slot antenna," *IEEE Trans. Antennas Propag.*, vol. 59, no. 5, pp. 1720–1724, May 2011.

[29] *Cubesat 101, Basic Concepts and Processes for First-Time Cubesat Developers*, NASA, Washington, DC, USA, 2017.

[30] "AZUR SPACE." Accessed: Mar. 1, 2024. [Online]. Available: https://www.azurspace.com

MAHMOUD N. MAHMOUD was born in Alexandria, Egypt. He received the B.Sc. degree in electrical engineering from Alexandria University, and the M.S. degree from the Department of Electrical and Computer Engineering, Utah State University. His major interests lie in the field of electromagnetics, antennas, and wireless communication systems.

REYHAN BAKTUR (Senior Member, IEEE) received the B.S. degree in electrical and electronics engineering from Tsinghua University, Beijing, China, in 1998, and the Ph.D. degree in electrical and computer engineering from Clemson University, Clemson, SC, USA, in 2005.

She joined the Department of Electrical and Computer Engineering, Utah State University, Logan, UT, USA, in 2006, where she is currently an Associate Professor. Her research interests include antenna design for CubeSats, optically transparent antennas, and integrated solar panel antennas. She is an IEEE Distinguished Lecturer in 2022–2024.